Flat bands and $\mathcal{PT}$ symmetry in quasi-one-dimensional lattices

Mario I. Molina
Department of Physics, MSI-Nucleus on Advanced Optics, and Center for Optics and Photonics, Faculty of Sciences, University of Chile, 7800003 Santiago, Chile
(Received 7 October 2015; published 8 December 2015)

We examine the effect of adding $\mathcal{PT}$-symmetric gain and loss terms to quasi-one-dimensional lattices (ribbons) that possess flat bands. We focus on three representative cases: the Lieb ribbon, the kagome ribbon, and the stub ribbon. In general, we find that the effect on the flat band depends strongly on the geometrical details of the lattice being examined. One interesting result that emerges from an analytical calculation of the band structure of the Lieb ribbon including gain and loss is that its flat band survives the addition of $\mathcal{PT}$ symmetry for any amount of gain and loss and also survives the presence of anisotropic couplings. For the other two lattices, any presence of gain and loss destroys their flat bands. For all three ribbons, there are finite stability windows whose size decreases with the strength of the gain and loss parameter. For the Lieb and kagome cases, the size of this window converges to a finite value. The existence of finite stability windows plus the constancy of the Lieb flat band are in marked contrast to the behavior of a pure one-dimensional lattice.

DOI: 10.1103/PhysRevA.92.063813 PACS number(s): 42.25.−p, 63.20.Pw, 42.82.Et, 78.67.Pt

I. INTRODUCTION

The concept of parity-time ($\mathcal{PT}$) symmetry has gained considerable attention in recent years. It started with the seminal work of Bender *et al.* [1,2], who demonstrated that non-Hermitian Hamiltonians are capable of displaying a purely real eigenvalue spectrum when the system is invariant with respect to the combined operations of parity and time-reversal symmetry. When applied to one-dimensional systems, the $\mathcal{PT}$ symmetry requires that the imaginary part of the potential term in the Hamiltonian be an odd function and its real part be even. In a $\mathcal{PT}$-symmetric system, the effects of loss and gain can balance each other and as a result give rise to a bounded dynamics. The system thus described can experience a spontaneous symmetry breaking from a $\mathcal{PT}$-symmetric phase (all eigenvalues real) to a broken phase (at least two complex eigenvalues) as the imaginary part of the potential is increased.

In the case of optics, the paraxial wave equation is formally identical to a Schrödinger equation and as a consequence the potential is proportional to the index of refraction. In this context, the $\mathcal{PT}$-symmetry requirements translates into the condition that the real part of the refractive index be an even function and the imaginary part be an odd function in space.

To date, numerous $\mathcal{PT}$-symmetric systems have been explored in several fields, including optics [3–8], electronic circuits [9], solid-state and atomic physics [10,11], and magnetic metamaterials [12]. The $\mathcal{PT}$-symmetry-breaking phenomenon has also been observed in several experiments [6,7,13,14]. It has been shown that a one-dimensional simple periodic lattice with homogeneous couplings and endowed with gain and loss obeying $\mathcal{PT}$ symmetry is always in the broken phase of this symmetry and does not have a stable parameter window [15]. However, for finite $\mathcal{PT}$-symmetrical lattices with homogeneous couplings, it has been shown that $\mathcal{PT}$ symmetry is preserved inside a parameter window whose size shrinks with the number of lattice sites [16]. Considering an infinite binary lattice, if one breaks the homogeneity of the couplings, it was shown that there is a well-defined parameter window where $\mathcal{PT}$ symmetry is preserved [17].

On the other hand, Hermitian systems that exhibit flat bands have attracted considerable interest, including optical [18,19] and photonic lattices [20–22], graphene [23,24], superconductors [25–28], fractional quantum Hall systems [29–31], and exciton-polariton condensates [32,33]. The presence of a flat band in the spectrum of a Hermitian lattice implies the existence of a set of entirely degenerate states whose superposition displays no dynamical evolution. This allows the formation of compactonlike structures that are completely localized in space, constituting a different form of localized state in the continuum. Such states have been recently observed experimentally in an optical waveguide array forming a Lieb lattice in the transversal direction [21,22]. This raises the possibility that a judicious superposition of these compactonlike states can be used to generate a whole set of diffraction-free modes that can carry information for long distances in an optical waveguide array. It becomes interesting then to examine the robustness of these localized modes under the presence of balanced loss and gain, obeying $\mathcal{PT}$ symmetry. The simplest optical lattice that is not strictly one dimensional and where one can have $\mathcal{PT}$ symmetry is a quasi-one-dimensional one with homogeneous couplings, i.e., a ribbon [34].

In this work we study analytically and numerically the spectrum and localization properties of three quasi-one-dimensional optical lattices with flat bands (Lieb, kagome, and stub) and how their spectra are affected by the presence of gain and loss terms that are $\mathcal{PT}$ symmetric. As we will see, the effect depends strongly on the particulars of the topology of the ribbon being studied. While in the case of the stub and kagome ribbons the presence of gain and loss destroys the flat bands, in the case of the Lieb ribbon we show analytically that its flat band remains unaltered no matter how large the strength of the gain and loss terms is. It even survives the case with anisotropic couplings.

II. MODEL

Let us consider a quasi-one-dimensional lattice (ribbon) representing, for example, a cross section of an optical

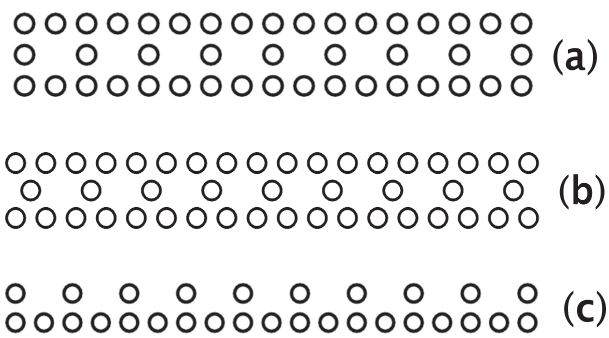

FIG. 1. (a) Lieb, (b) kagome, and (c) stub ribbons, with homogeneous coupling and in the absence of $\mathcal{PT}$ symmetry. They have infinite extension along the horizontal direction.

waveguide array (see Fig. 1). In this context and in the coupled-mode framework, the evolution of the electric field on guide $\mathbf{n}$ is given by [35]

$$i\frac{d}{dz}C_{\mathbf{n}}(z) + i\rho_{\mathbf{n}} + V\sum_{\mathbf{m}} C_{\mathbf{m}}(z) = 0, \tag{1}$$

where $C_{\mathbf{n}}(z)$ is proportional to the amplitude of the electric field at site $\mathbf{n}$, z is the propagation coordinate, $\rho_{\mathbf{n}}$ is the gain and loss coefficient on site $\mathbf{n}$, V is the coupling among waveguides, and the sum in Eq. (1) is restricted to nearest neighbors only. Stationary modes are obtained from the ansatz $C_{\mathbf{n}}(z) = C_{\mathbf{n}}\exp(i\lambda z)$, where the $C_{\mathbf{n}}$ amplitudes obey

$$-\lambda C_{\mathbf{n}} + i\rho_{\mathbf{n}} + V\sum_{\mathbf{m}} C_{\mathbf{m}} = 0, \tag{2}$$

where λ is the propagation constant of the mode. Figure 1 shows three examples of ribbons that will be considered in this work. The presence of $\rho_{\mathbf{n}}$ leads, in general, to an exponential increase or decrease of the amplitude $C_{\mathbf{n}}$ as the mode evolves in time z. However, as mentioned in the Introduction, there are special cases where the gain and loss terms can be balanced so that the dynamics remain bounded. Such is the case of a $\mathcal{PT}$-symmetric configuration where the value of $\rho_{\mathbf{n}}$ is an odd function in space. The gain and loss terms of the three ribbons shown in Fig. 1 can be set up to obey this condition. What we want to know is the effect of adding $\mathcal{PT}$ symmetry to those ribbons that originally possess flat bands. To accomplish this, we examine the spectra of these ribbons as well as the average participation ratio of the states $\langle P\rangle = \langle(\sum_n |C_n|^2)^2/\sum_n |C_n|^4\rangle$, where the average is over all states, for a given $\rho_{\mathbf{n}}$ distribution. Here $\langle P\rangle$ provides a rough measure of localization tendency. For a completely localized state $\langle P\rangle = 1$, while for a completely delocalized state $\langle P\rangle = N$.

A. Lieb ribbon

The Lieb ribbon is shown in Fig. 1(a). It consists essentially of a depleted square lattice ribbon. Its unitary cell contains five units. In the absence of gain and loss ($\rho_{\mathbf{n}} = 0$), one obtains five bands

$$\begin{aligned} \lambda &= 0,\\ \lambda &= \pm\sqrt{2[1+\cos(2k)]}V, \\ \lambda &= \pm\sqrt{4+2\cos(2k)}V. \end{aligned} \tag{3}$$

Thus, out of the five bands, we have the flat band $\lambda = 0$. The modes belonging to this band have zero group velocity, which leads to a sharp transverse localization. These compacton-like modes are able to propagate along the guide without diffraction. The reason for this localization is a geometric phase cancellation among nearby sites. Some examples of such modes can be found in Ref. [36]. The addition of a small amount of $\mathcal{PT}$ symmetry in a perturbative manner has been examined in Ref. [37].

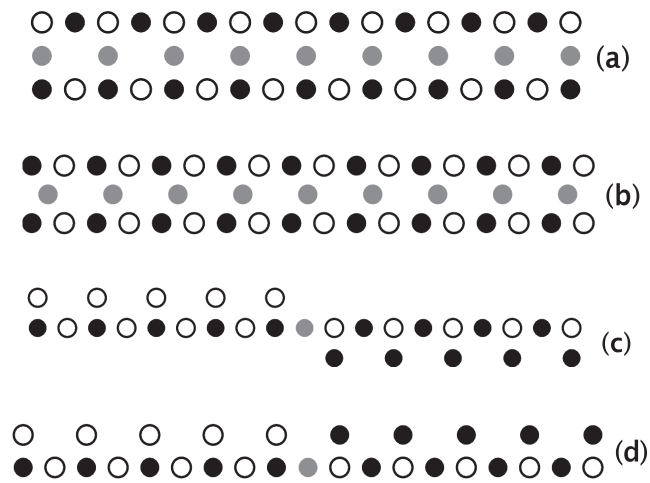

FIG. 2. Ribbons with $\mathcal{PT}$ symmetry: (a) $\mathcal{PT}$-symmetric Lieb ribbon, (b) $\mathcal{PT}$-symmetric kagome ribbon, (c) $\mathcal{PT}$-symmetric stub ribbon, and (d) topologically equivalent $\mathcal{PT}$-symmetric stub ribbon. Black (white) circles denote loss (gain), while the gray circles represent the absence of gain and loss.

Here, however, we incorporate an arbitrary amount of $\mathcal{PT}$-symmetric gain and loss into the system. There are several ways to achieve this and we take the simplest one, depicted in Fig. 2(a). For this configuration the five coupled equations incorporating $\mathcal{PT}$ symmetry lead to the five complex bands

$$\begin{aligned} \lambda &= 0,\\ \lambda &= \pm\sqrt{2(1+\cos(2k))V^2-\rho^2}, \\ \lambda &= \pm\sqrt{(4+2\cos(2k))V^2-\rho^2}. \end{aligned} \tag{4}$$

As we can see, the flat band $\lambda = 0$ still remains and is therefore unaltered by the presence of $\mathcal{PT}$-symmetric gain and loss terms. Two of the other four (dispersive) bands are real for $0 < \rho < \sqrt{2}$, while the other two contain imaginary eigenvalues for any ρ value. Thus, as soon as ρ is different from zero, the whole system is in the broken-$\mathcal{PT}$-symmetry phase.

The flat band also survives the addition of anisotropic couplings: If we denote by V_x (V_y) the coupling in the horizontal (vertical) direction, then the five bands will be given

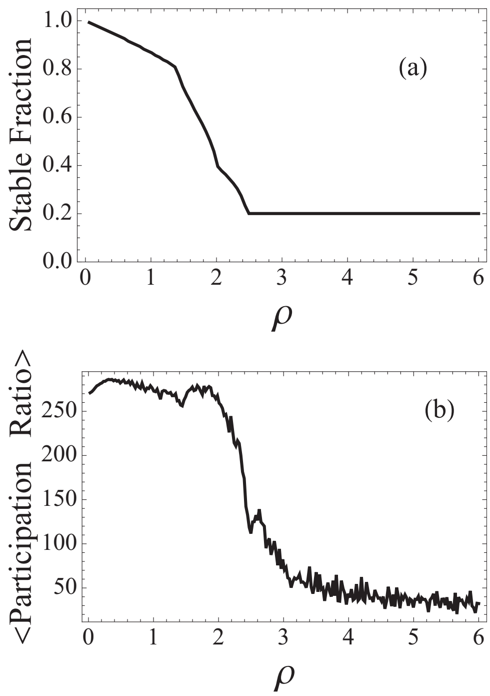

FIG. 3. Lieb ribbon. (a) Fraction of stable modes $\text{Im}[\lambda] = 0$ as a function of the gain and loss parameter. (b) Average of the participation ration over all stable states, as a function of the gain and loss parameter. The total number of sites $N = 543$.

by

$$\begin{aligned} \lambda &= 0, \\ \lambda &= \pm\sqrt{2(1+\cos(2k))V_x^2 - \rho^2}, \\ \lambda &= \pm\sqrt{2\left(V_x^2 + V_y^2\right) + 2V_x^2\cos(2k) - \rho^2} \end{aligned} \tag{5}$$

and the flat band $\lambda = 0$ is still there.

Let us now concentrate on the fraction of stable states (i.e., $\text{Im}[\lambda] = 0$), that is, the fraction with purely real eigenvalues. We can anticipate that, as the gain and loss parameter ρ is increased, this fraction will decrease and at large ρ values will approach a constant value stemming from the flat band states (which are stable). They constitute $1/5$ of the total number of states. Thus the stable fraction should approach asymptotically a value of 0.2. Figure 3 shows the stable fraction and the average (over stable states) of the participation ratio $\langle P \rangle$ as a function of the gain and loss parameter. While at small values of ρ the $\langle P \rangle$ stays nearly constant, it begins to decay rapidly past $\rho \sim 2V$ accompanied by large oscillations. The steady decrease of $\langle P \rangle$ with ρ indicates an overall tendency towards localization as the gain and loss parameter is increased.

B. Kagome ribbon

The kagome ribbon is shown in Fig. 1(b). This geometry has been used in the past in studies of magnetization in frustrated quantum lattices [38]. This ribbon has five sites in its unit cell, which implies five bands. In the absence of gain and loss

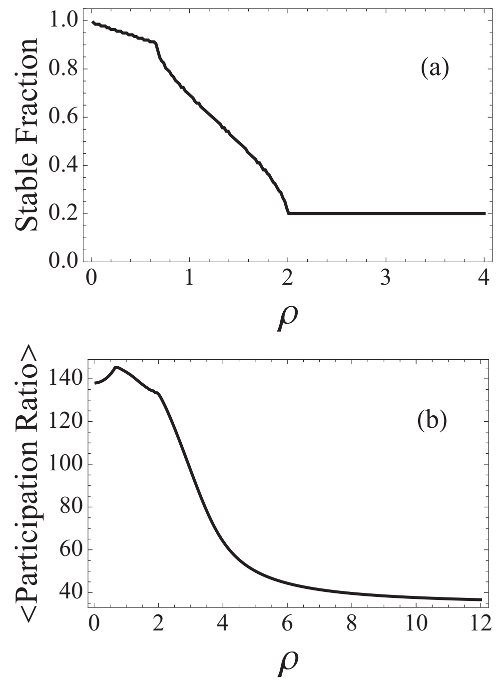

FIG. 4. Kagome ribbon. (a) Fraction of stable modes $\text{Im}[\lambda] = 0$ as a function of the gain and loss parameter. (b) Average of the participation ratio over all stable states, as a function of the gain and loss parameter. The total number of sites $N = 275$.

($\rho_{\mathbf{n}} = 0$) they are given by

$$\begin{aligned} \lambda &= -2V, \\ \lambda &= \pm\sqrt{2[1+\cos(2k)]}V, \\ \lambda &= [1 \pm \sqrt{3 + 2\cos(2k)}]V. \end{aligned} \tag{6}$$

Thus, we have the flat band $\lambda = -2V$. When gain and loss are added, it is no longer possible to extract the bands in closed form as we did for the Lieb lattice. A numerical examination of all eigenvalues reveals that as soon as $\rho_{\mathbf{n}}$ differs from zero, the flat band is lost and also complex eigenvalues appear, that is, the system enters the broken-$\mathcal{PT}$-symmetry phase. The fraction of stable states, that is, those states with $\text{Im}[\lambda] = 0$, and their participation ratios $\langle P \rangle$ as a function of the gain and loss parameter ρ are shown in Fig. 4. The general tendency of Figs. 3 and 4 is the same. In both cases the stable fraction and the participation ratio decrease with ρ. Since in this case we no longer have a flat band, the asymptotic fraction of stable states is only due to the presence of a finite percentage of states with $\text{Im}[\lambda] = 0$.

C. Stub ribbon

The stub ribbon is shown in Fig. 1(c). Its geometry has been used in the past in studies on boson and fermion dynamics [19]. Its unitary cell has three sites. In the absence of gain and loss, this leads to three real bands

$$\lambda = 0, \quad \lambda = \pm\sqrt{3 + 2\cos(2k)}V, \tag{7}$$

where, as in the Lieb case, we have a flat band at $\lambda = 0$. A simple $\mathcal{PT}$-symmetric configuration for this lattice is shown in Fig. 2(c). It is topologically equivalent to the one shown

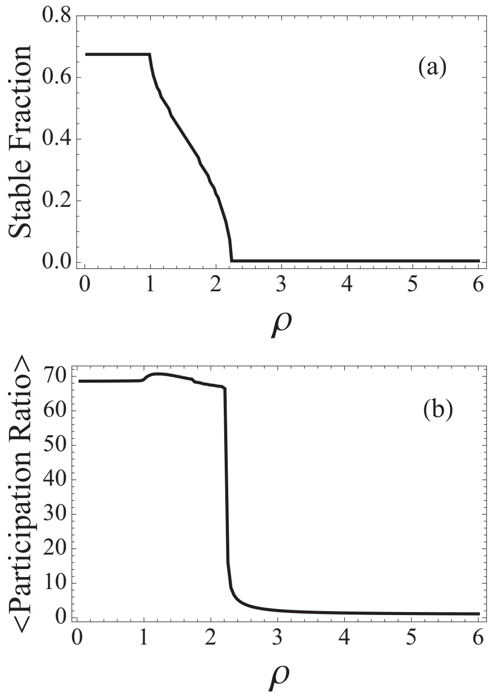

FIG. 5. Stub ribbon: (a) Fraction of stable modes $\text{Im}[\lambda] = 0$ as a function of the gain and loss parameter. (b) Average of the participation ratio over all stable states, as a function of the gain and loss parameter. The total number of sites $N = 203$.

in Fig. 2(d). As we can see, roughly speaking, the lattice has been split into two halves and a closed-form calculation of the eigenvalues from Eq. (2) is not possible. Numerical examination of all eigenvalues for varying ribbon lengths reveals that the flat band disappears as soon as ρ is different from zero and complex eigenvalues appear, causing the system to enter the broken-$\mathcal{PT}$-symmetry phase.

The stable fraction [shown in Fig. 5(a)] has an interesting behavior: It remains constant until a first critical ρ value is reached. Then it drops with an increase in ρ reaching the value $1/N$, where N is the total number of sites, at a second critical value. There the system undergoes a spontaneous $\mathcal{PT}$-symmetry breaking and the eigenvalues are no longer purely real (in the limit of an infinite ribbon $N \to \infty$). On the other hand, the participation ratio [shown in Fig. 5(b)] $\langle P \rangle$ remains more or less constant with an increase in ρ, until reaching the second critical ρ value mentioned before, where it drops abruptly, converging to unity at large gain and loss values. In this case we see an abrupt transition of the stable modes from relatively extended (on average) to highly localized.

III. CONCLUSION

In this work we have examined the spectral properties of several quasi-one-dimensional optical lattices (Lieb, kagome, and stub) that, in the absence of gain and loss, feature a flat band. We have incorporated $\mathcal{PT}$-symmetric gain and loss terms and examined the changes in their spectra. The results show that while there are common trends for all of them, there are also features that are present only in each case. Perhaps the most interesting analytical result is that a Lieb ribbon maintains its flat band, regardless of the strength of the gain and loss term and the presence of anisotropic couplings. This is quite surprising since usually the addition of $\mathcal{PT}$-symmetry leads to a stability window that shrinks with the strength of gain and loss. However, for the Lieb lattice, the system not only remains stable, but keeps its original flat band for any $\mathcal{PT}$-symmetric gain and loss amount. A common feature for the three cases is the presence of a finite stable fraction (in the infinite ribbon length) that decreases with the increase in gain and loss. While for the Lieb and kagome ribbons this fraction remain finite at large values of gain and loss, for the stub lattice it vanishes at a certain ρ value and the system enters the broken-$\mathcal{PT}$-symmetry regime. The average participation value of all ribbons also decreases with an increase in gain and loss, reaching a finite value at high-ρ values. For the stub lattice in particular, the $\langle P \rangle$ approaches unity. Now, this $\langle P \rangle$ is a rough estimate and only measures the general tendency towards localization. As the gain and loss parameter ρ increases, the stationary wave function seems to concentrate more and more power ($\sum_n |C_n|^2$) at certain sites causing the decrease in $\langle P \rangle$. As long as this power concentration is finite, the system will be dynamically stable.

We conclude that the spectral properties of a given ribbon depend on its geometry and that the addition of $\mathcal{PT}$ symmetry to a ribbon possessing a flat band will result in most cases in a complete destruction of its flat band. An exception to this behavior is the Lieb ribbon, where its flat band shows a remarkable robustness to $\mathcal{PT}$ symmetry. This feature isolates the Lieb ribbon as a possible candidate for a stable long-distance image transmission system. Its quasi-one-dimensional geometry makes its fabrication possible by means of the laser-written waveguide technique [39].

ACKNOWLEDGMENTS

This work was partially supported by FONDECYT Grant No. 1120123, Programa ICM No. P10-030-F, and Programa de Financiamiento Basal de CONICYT (No. FB0824/2008).

[1] C. M. Bender and S. Boettcher, Phys. Rev. Lett. **80**, 5243 (1998).

[2] C. M. Bender, D. C. Brody, and H. F. Jones, Phys. Rev. Lett. **89**, 270401 (2002).

[3] R. El-Ganainy, K. G. Makris, D. N. Christodoulides, and Z. H. Musslimani, Opt. Lett. **32**, 2632 (2007).

[4] Z. H. Musslimani, K. G. Makris, R. El-Ganainy, and D. N. Christodoulides, Phys. Rev. Lett. **100**, 030402 (2008).

[5] K. G. Makris, R. El-Ganainy, D. N. Christodoulides, and Z. H. Musslimani, Phys. Rev. Lett. **100**, 103904 (2008).

[6] A. Guo, G. J. Salamo, D. Duchesne, R. Morandotti, M. Volatier-Ravat, V. Aimez, G. A. Siviloglou, and D. N. Christodoulides, Phys. Rev. Lett. **103**, 093902 (2009).

[7] C. E. Rüter, K. G. Makris, R. El-Ganainy, D. N. Christodoulides, M. Segev, and D. Kip, Nat. Phys. **6**, 192 (2010).

[8] A. Regensburger, C. Bersch, M. A. Miri, G. Onishchukov, D. N. Christodoulides, and U. Peschel, Nature (London) **488**, 167 (2012).
[9] J. Schindler, A. Li, M. C. Zheng, F. M. Ellis, and T. Kottos, Phys. Rev. A **84**, 040101 (2011).
[10] N. Hatano and D. R. Nelson, Phys. Rev. Lett. **77**, 570 (1996).
[11] Y. N. Joglekar, D. Scott, M. Babbey, and A. Saxena, Phys. Rev. A **82**, 030103(R) (2010).
[12] N. Lazarides and G. P. Tsironis, Phys. Rev. Lett. **110**, 053901 (2013).
[13] A. Szameit, M. C. Rechtsman, O. Bahat-Treidel, and M. Segev, Phys. Rev. A **84**, 021806 (2011).
[14] A. E. Miroshnichenko, B. A. Malomed, and Y. S. Kivshar, Phys. Rev. A **84**, 012123 (2011).
[15] G. Tsironis and N. Lazarides, Appl. Phys. A **115**, 449 (2014).
[16] M. I. Molina, Phys. Rev. E **89**, 033201 (2014).
[17] S. V. Dmitriev, A. A. Sukhorukov, and Y. S. Kivshar, Opt. Lett. **35**, 2976 (2010).
[18] V. Apaja, M. Hyrkäs, and M. Manninen, Phys. Rev. A **82**, 041402(R) (2010).
[19] M. Hyrkäs, V. Apaja, and M. Manninen, Phys. Rev. A **87**, 023614 (2013).
[20] M. C. Rechtsman, J. M. Zeuner, A. Tünnermann, S. Nolte, M. Segev, and A. Szameit, Nat. Photon. **7**, 153 (2013).
[21] R. A. Vicencio, C. Cantillano, L. Morales-Inostroza, B. Real, C. Mejía-Cortés, S. Weimann, A. Szameit, and M. I. Molina, Phys. Rev. Lett. **114**, 245503 (2015).
[22] S. Mukherjee, A. Spracklen, D. Choudhury, N. Goldman, P. Öhberg, E. Andersson, and R. R. Thomson, Phys. Rev. Lett. **114**, 245504 (2015).
[23] C. L. Kane and E. J. Mele, Phys. Rev. Lett. **78**, 1932 (1997).
[24] F. Guinea, M. I. Katsnelson, and A. K. Geim, Nat. Phys. **6**, 30 (2010).
[25] A. Simon, Angew. Chem. **109**, 1873 (1997).
[26] S. Deng, A. Simon, and J. Köhler, Angew. Chem. **110**, 664 (1998).
[27] S. Deng, A. Simon, and J. Köhler, J. Solid State Chem. **176**, 412 (2003).
[28] M. Imada and M. Kohno, Phys. Rev. Lett. **84**, 143 (2000).
[29] E. Tang, J.-W. Mei, and X.-G. Wen, Phys. Rev. Lett. **106**, 236802 (2011).
[30] T. Neupert, L. Santos, C. Chamon, and C. Mudry, Phys. Rev. Lett. **106**, 236804 (2011).
[31] S. Yang, Z.-C. Gu, K. Sun, and S. Das Sarma, Phys. Rev. B **86**, 241112(R) (2012).
[32] T. Jacqmin, I. Carusotto, I. Sagnes, M. Abbarchi, D. D. Solnyshkov, G. Malpuech, E. Galopin, A. Lemaitre, J. Bloch, and A. Amo, Phys. Rev. Lett. **112**, 116402 (2014).
[33] F. Baboux, L. Ge, T. Jacqmin, M. Biondi, A. Lematre, L. Le Gratiet, I. Sagnes, S. Schmidt, H. E. Türeci, A. Amo, and J. Bloch, arXiv:1505.05652.
[34] M. I. Molina, Phys. Lett. A **376**, 3458 (2012).
[35] See, for example, P. G. Kevrekidis, *The Discrete Nonlinear Schrödinger Equation* (Springer, Berlin, 2009).
[36] D. López-González and M. I. Molina (unpublished).
[37] L. Ge, Phys. Rev. A **92**, 052103 (2015).
[38] J. Schulenburg, A. Honecker, J. Schnack, J. Richter, and H.-J. Schmidt, Phys. Rev. Lett. **88**, 167207 (2002); O. Derzhko, J. Richter, A. Honecker, M. Maksymenko, and R. Moessner, Phys. Rev. B **81**, 014421 (2010).
[39] T. Eichelkraut *et al.*, Nat. Commun. **4**, 2533 (2013).